International Journal of Remote Sensing
Vol. 27, No. 19, 10 October 2006, 4245–4266

Taylor & Francis
Taylor & Francis Group

Irrigated area mapping in heterogeneous landscapes with MODIS time series, ground truth and census data, Krishna Basin, India

T. W. BIGGS*†‡, P. S. THENKABAIL§, M. K. GUMMA†, C. A. SCOTT¶, G. R. PARTHASARADHI† and H. N. TURRAL§

†International Water Management Institute, South Asia Regional Office, Patancheru, Andhra Pradesh, India, 502-324

‡INTERA Incorporated, PO Box 818, Niwot, Colorado, USA, 80544

§International Water Management Institute, Headquarters, Colombo, Sri Lanka

¶Department of Geography and Regional Development, University of Arizona, Tucson, AZ 85721

(*Received 26 April 2005; in final form 19 July 2005*)

Diverse irrigated areas were mapped in the Krishna River Basin (258,912 km^2), southern India, using an irrigated fraction approach and multiple ancillary data sources. Unsupervised classification of a monthly time series of net difference vegetation index (NDVI) images from the Moderate Resolution Imaging Spectrometer (MODIS) over January–December 2002 generated 40 classes. Nine generalized classes included five irrigated classes with distinct NDVI time signatures: continuous irrigation, double-cropped, irrigated with low biomass, minor irrigation, and groundwater irrigation. Areas irrigated by surface water began greening 45 days after groundwater-irrigated areas, which allowed separation of surface and groundwater irrigation in the classification. The fraction of each class area irrigated was determined using three different methods: ground truth data, a linear regression model calibrated to agricultural census data, and visual interpretation of Landsat TM imagery. Irrigated fractions determined by the three methods varied least for the double-cropped irrigated class (0.62–0.79) and rangeland (0.00–0.02), and most for the minor irrigated class (0.06–0.43). Small irrigated patches ($<0.1\,km^2$) accounted for more irrigated area than all major surface water irrigated areas combined. The irrigated fractions of the minor and groundwater-irrigated classes differed widely by method, suggesting that mapping patchy and small irrigated areas remains challenging, but comparison of multiple data sources improves confidence in the classification and highlights areas requiring more intensive fieldwork.

1. Introduction

Irrigated areas account for 84% of global water use by humans (Shiklomanov 2000), and can affect regional and even global hydrological processes (Rosenberg 2000). Irrigated area mapping forms an important part of basin characterization, hydrological modeling, and agricultural planning, but significant technical challenges remain for producing robust irrigated area maps. Farmers irrigate a diverse range of plot sizes, crops, and water sources, which complicates the use of simple rules to map irrigated areas from satellite imagery. Irrigated lands also

*Corresponding author. Email: trentbren@yahoo.com

International Journal of Remote Sensing
ISSN 0143-1161 print/ISSN 1366-5901 online
http://www.tandf.co.uk/journals
DOI: 10.1080/01431160600851801

include a spectrum of command area sizes, from major, contiguous canal-irrigated systems, to areas irrigated by small reservoirs, to individual groundwater-irrigated plots (Droogers 2002). Groundwater irrigation, in particular, has become increasingly common globally. In India, the total groundwater-irrigated area exceeds the surface-irrigated area (Shah *et al*. 2000). Most groundwater-irrigated plots are small (<1 ha), which complicates use of traditional satellite image classification techniques, particularly for regional mapping. Identification of training sites for supervised classifications is particularly problematic in areas with patchy irrigated systems, where plot sizes are often small relative to satellite pixels.

Accuracy assessment of irrigated area maps over large areas is also difficult where irrigated areas are small relative to the satellite image pixel. Traditional accuracy assessment involves collection of ground truth points which are assigned discrete classes and compared with a classified image with discrete classes. Only a small fraction of the land surface in a large basin can be visited by traditional ground truth campaigns, and accuracy assessments that assign discrete classes to pixels can be misleading and inappropriate where plot sizes are small relative to the pixel size (Friedl *et al*. 2000). Determination of the fraction of an area covered by a particular land cover, rather than classification into discrete categories, may be the most appropriate way of mapping and assessing accuracy for regional maps generated from coarse resolution imagery (Latifovic and Olthof 2004). Other non-traditional techniques, such as use of higher resolution imagery to validate coarse-resolution maps, can also be used in place of ground truth data over large areas (DeFries *et al*. 1998).

In addition to field surveys for accuracy assessment, agricultural census data collected by government agencies have been used to check and enhance satellite-based mapping of large areas (Ramankutty and Foley 1998, Walker and Mallawaarachichi 1998, Cardille and Foley 2003), including irrigated areas (Frolking *et al*. 2002). The quality of agricultural census data is often called into question (Droogers 2002). In India, agricultural census data are internally consistent and generally thought to be accurate, though their overall accuracy has not been well documented (Guilmoto 2002). The comparison of several different methods for mapping irrigated areas, as we propose and implement here, can either enhance confidence in the final map accuracy or highlight areas needing further validation.

Regional mapping of irrigated areas also should account for a wide range of crops, water delivery systems, and cropping calendars. Multi-cropping and varying cropping calendars make single-image snap-shots inadequate for characterizing the full range of irrigated areas (Sellers and Schimel 1993). Many crops have relatively short and staggered growth, development, and senescent phases, making accurate mapping difficult using satellite images from a single or even a series of overpasses. Time series of satellite imagery and indices derived from them, such as the net difference vegetation index (NDVI), can be used for mapping vegetation phenology (Reed *et al*. 1994), image classification (Lloyd 1990, DeFries and Townshend 1994, Moody and Johnson 2001), crop parameter identification (Fischer 1994) and yield estimation (Hill and Donald 2003). NDVI time series have not been used to investigate regional variations in cropping patterns of irrigated areas and to separate surface- and groundwater-irrigated areas (but see Wardlow and Egbert 2002). The large scene size and daily overpass rate of the Moderate Resolution Imaging Spectrometer (MODIS) make it attractive for large area crop mapping, and NDVI derived from MODIS has high fidelity with biophysical parameters (Huete *et al*.

2002). While other bands of the MODIS satellite may be used to improve a classification, such as thermal or mid-infrared, these other bands capture features of the landscape that are not easy to interpret, require resource-intensive field plot data, correlate with NDVI, and may subset landscapes into additional units not relevant to irrigated area mapping. Use of NDVI time series as an indicator of vegetation phenology consumes less storage, saves processing time, and provides a simple classification of complex landscapes.

This paper presents maps of land cover and irrigated areas in a heterogeneous landscape dominated by smallholder agriculture using NDVI time series and an irrigated fraction approach. The method fuses and compares multiple data sources, including a time series of MODIS imagery, ground truth data, agricultural census data, and Landsat TM imagery. First, generalized classes of land cover are generated using unsupervised classification of a time series of MODIS NDVI images. Irrigated fractions and total irrigated area for each remote sensing class are then estimated using three methods: ground truth data, linear regression on agricultural census data, and Landsat imagery. Accuracy assessment is performed by comparing the irrigated fraction statistics determined by each data source, and by fuzzy accuracy assessment on ground truth data (Thenkabail *et al.* 2005). A logistic model of vegetation phenology is used to define vegetation growth stages. The main innovations of the method include the use of NDVI time series to identify and classify diverse irrigated areas, including separation of areas irrigated by surface water and groundwater, and the use of multiple ancillary data sources including census data for aggregate accuracy assessment.

2. Study area

The Krishna Basin is the fourth largest river basin in India (258 912 km^2; figure 1). The Krishna River originates in the Western Ghats mountains, flows east across the Deccan Plateau, and discharges into the Bay of Bengal. The Krishna River has three main tributaries that drain from the northwest, west, and southwest. The climate is semi-arid in the central part of the basin, sub-humid in the eastern delta, and sub-humid to humid in the Western Ghats. Annual precipitation averages 780 mm and decreases with distance inland from 850–1000 mm in the Krishna Delta to 300–400 mm in the northwest. In the extreme western parts of the basin, the Western Ghats have high annual precipitation (1500–2500 mm). Most of the rainfall in the basin occurs during the monsoon from June to October.

Cropping occurs in three seasons: Kharif during the monsoon (June to November), Rabi in the post-monsoon (December–March) and a summer season in April and May. Most farmers leave fields fallow during the summer season due to lack of rain and irrigation water. Irrigated areas include double cropping of rice and grains, single cropping of sugarcane, chili, and fodder grass, and some areas of light or supplemental irrigation of cotton, oilseeds, corn, sorghum, and other grains. Single cropping of rice is common in areas irrigated by groundwater. Other irrigated crops include bananas, vegetables, ginger, turmeric, and teak, but they occupy relatively small fractions of the total irrigated area. Rainfed crops include grains (sorghum, millet), pulses (red and green gram, chickpea), and oilseeds (sunflower, groundnut).

Irrigation systems include major (>10 000 ha), medium (20–10 000 ha), and minor (<20 ha) command areas. Major canal irrigated projects have been built along each

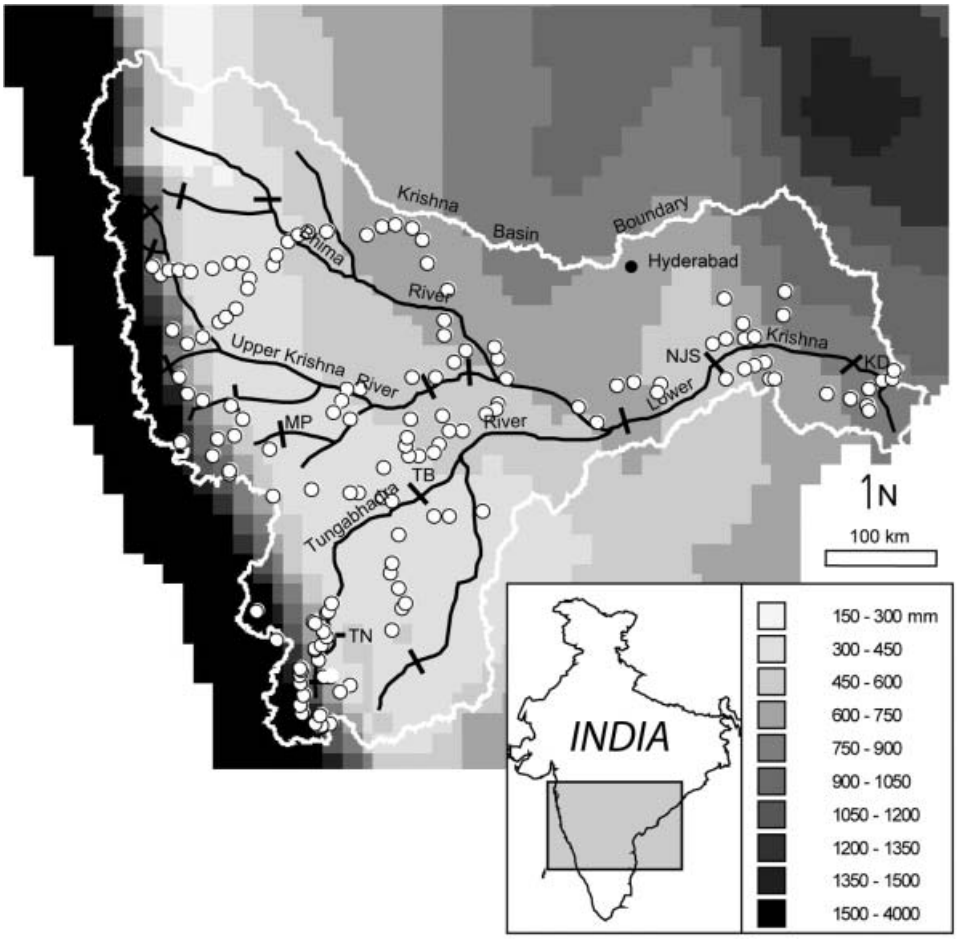

Figure 1. Location map of the Krishna Basin, showing average annual rainfall (mm), and ground truth points from the October 2003 field campaign (white circles). Dark lines perpendicular to streams indicate major dams. MP=Malaphrabha Dam, TB=Tungabhadra Dam, NJS=Nagarjuna Sagar Dam, KD=Krishna Delta Anicut, TN=Tunga Dam.

of the three main tributaries in the upper basin, along the main stem in the lower basin, and in the delta (figure 1). Numerous smaller reservoirs at the base of the Western Ghats supply canal-irrigated projects in the upper Krishna Basin. Minor irrigation includes small reservoirs, riparian lift schemes, and groundwater irrigation from dug wells, shallow tube wells, and deep tube wells. Small reservoirs are used for both surface irrigation and groundwater recharge.

3. Methods

3.1 *NDVI time series classification*

A time series of MODIS 8-day composite reflectance images, 500-m resolution, was obtained for 8 January–31 December 2002 (MOD09A1 data product). There were three to four 8-day composites per month for a total of 45 8-day composites. The MOD09A1 data set is free of cost, pre-calibrated, and cleaned for cloud effects using the maximum NDVI method (Holben 1986, King *et al.* 2003, http://modis-sr.

ltdri.org/html/intro.htm). Monthly maximum value composites (MVCs) for January through December were created using the 8-day images in order to minimize cloud effects during the monsoon season. The monthly MVCs were stacked into a 12-band NDVI MVC mega-file image (MFI).

Unsupervised classification followed by progressive generalization (Cihlar *et al.* 1998) was used to classify the MODIS time series. Unsupervised classification was used in order to capture the full range of NDVI time series over a large area, which is recommended for large areas that cover a wide and unknown range of vegetation types, and where landscape heterogeneity complicates identification of homogeneous training sites (Achard and Estreguil 1995, Cihlar 2000). Identification of training sites is particularly problematic for small, heterogeneous irrigated areas common in India.

The ISOCLASS cluster algorithm (ISODATA in ERDAS Imagine 8.7^{TM}) run on the MFI generated an initial 40 classes, with a maximum of 40 iterations and convergence threshold of 0.99. The initial 40 classes were merged by user-controlled progressive generalization (Cihlar *et al.* 1998) using the class-average NDVI time series, ground truth data (described below), and GeoCover Landsat imagery from 1990 and 2000 (Tucker *et al.* 2004). Classes with similar NDVI time series and land cover were merged into a single class, and classes showing significant mixing, e.g. continuous irrigated areas and forest, were masked and reclassified using the same ISOCLASS algorithm. Some continuous irrigated areas that mixed with forests in the Western Ghats were separated using a 90 m digital elevation model (DEM) from the Shuttle Radar Topography mission (SRTM) and an elevation threshold of 630 m, which was determined using the DEM, Landsat imagery and ground truth data. Progressive generalization resulted in a 37-class map and a 9-class map with class descriptions based on the ground truth data and visual interpretation of the Landsat TM imagery (table 1). While class aggregation could have been performed statistically using a Euclidean or other distance measure, the user-controlled method incorporates both ground truth and Landsat data in order to avoid lumping classes that might be spectrally similar but have distinct land cover. The NDVI of some classes differed in only one or two months, which would have caused the classes to be merged if an automated similarity index were used to merge the classes.

Ground truth data were collected at 140 locations in October 2003 covering the major crop regions of the basin (figure 1). Land cover, including percent cover of trees, shrubs, grasses, cropland, and irrigation sources was estimated visually at each location over a 90 m × 90 m plot representative of a large homogeneous area. Dominant crops were determined in the field and by interviews with local farmers.

3.2 *Irrigated fractions*

MODIS NDVI pixels are 500 m × 500 m, which is larger than many irrigated plots (figure 2). Due to this sub-pixel heterogeneity, each class in the unsupervised classification has both a name and an irrigated fraction. The area irrigated by surface or groundwater for a given area was computed from the MODIS classification as:

$$I_k = \sum_{i=1}^{n} \alpha_{i,k} A_i \tag{1}$$

where I_k is the net area irrigated by source k (surface or groundwater), i is the

Table 1. MODIS classes and vegetation cover statistics based on ground truth data. *N* is the number of ground truth points in each class. The 'Other' category includes a mix of built areas, fallow, weeds and rock.

				Vegetation cover percent (mean ± sd)						
Code	Description	Area (km^2)	*N*	Trees	Shrubs	Grass	Open/bare	Other	Crops	Dominant crops
1. WAT	Water bodies	2508	–	–	–	–	–		–	–
2. RL	Rangeland, wasteland mix rainfed crops	63 143	29	2 ± 2	10 ± 17	8 ± 8	13 ± 19	14 ± 25	53 ± 39	Grains, oilseeds
3. RFA	Rainfed crops, rangeland	51 162	25	3 ± 4	3 ± 4	11 ± 10	13 ± 19	17 ± 30	54 ± 37	Grains, oilseeds, pulses
4. RFG	Rainfed and ground water irrigation	62 944	32	3 ± 6	3 ± 7	7 ± 7	9 ± 17	7 ± 15	72 ± 29	Rice, grains, cotton, chili, oilseeds, pulses, vegetables
5. IMIN	Minor irrigation: riparian lift, tanks, groundwater	35 788	6	3 ± 3	3 ± 4	4 ± 3	6 ± 6	14 ± 30	70 ± 25	Rice, oilseeds, pulses, grains, cotton, chili
6. IL	Irrigated, low NDVI	7702	4	2 ± 2	2 ± 1	7 ± 9	3 ± 5	4 ± 6	83 ± 15	Cotton, grains, oilseeds, rice
7. ICONT	Irrigated, continuous	8600	10	3 ± 5	1.4 ± 0.8	4 ± 6	6 ± 12	6 ± 9	80 ± 23	Sugarcane, rice, fodder grass
8. IDBL	Irrigated, double crop	11 775	22	1.3 ± 1.0	1 ± 0.5	5 ± 9	1 ± 2	3 ± 3	89 ± 10	Rice, grains, pulses
9. FOR	Forests: evergreen, deciduous, mix shrubs	15 290	12	44 ± 32	11 ± 12	5 ± 4	11 ± 8	5 ± 7	25 ± 37	Teak, coffee, aracanut, rice
Basin total		258 912	144	5	4.9	7.3	9.6	12.2	61	

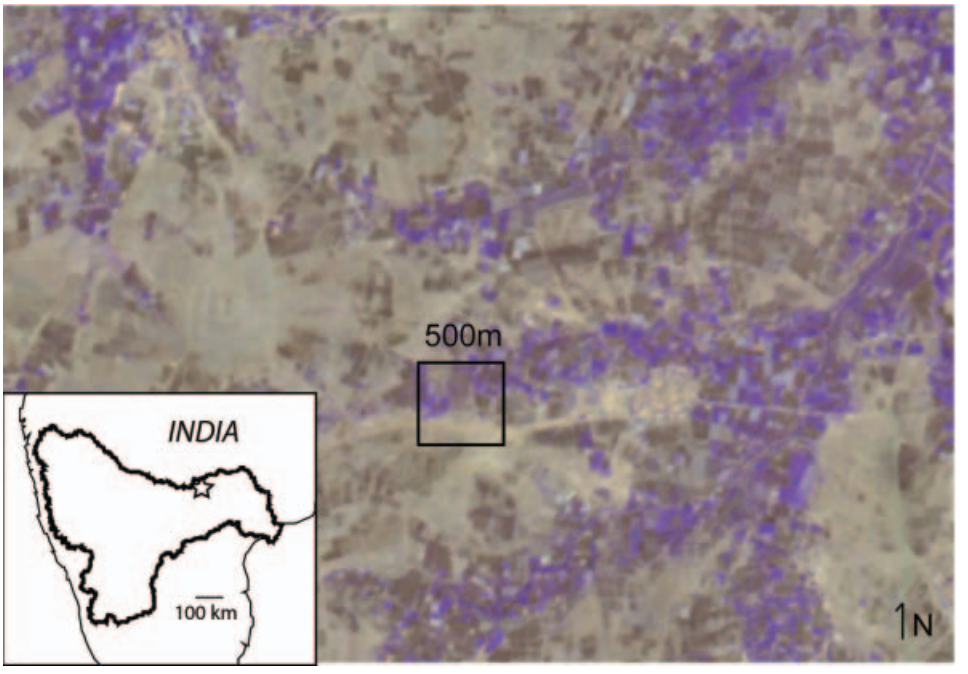

Figure 2. ASTER satellite image (15 m resolution) of a groundwater-irrigated mosaic in the north-central Krishna Basin taken at the end of the post-monsoon cropping season (3 March 2001). The black square on the image indicates the size of a single MODIS pixel. Brown and grey indicate rainfed cropland and rangelands, and purple indicates groundwater irrigation and some natural vegetation/trees.

MODIS class, n is the number of MODIS classes, $\alpha_{i,k}$ is the fraction of class i irrigated by source k, and A_i is the area covered by MODIS class i. Net irrigated area includes all places with an irrigated crop for one or more seasons during a year, and counts double-cropped areas once.

The irrigated fractions for each class ($\alpha_{i,k}$) were calculated using three methods: first as the average of the ground truth estimates (GT), second as coefficients in a multiple linear regression on census statistics (ML), and third using visual interpretation of Landsat TM imagery (TM). In the ML method, the $\alpha_{i,k}$ were the regression coefficients calibrated to net surface- or groundwater-irrigated area from the district-wise agricultural census (I_k) and class areas by district (A_i). Data on net irrigated area by source (I_k) were available for 23 administrative districts in the three basin States for 1997 and 1999 (figure 3). The district-irrigated area from the census was multiplied by the fraction of the district overlapping the basin. The multiple regressions were done with the intercept set to zero and step-wise to include only statistically significant classes ($p<0.05$).

Irrigated fractions based on Landsat TM imagery (TM method) were made by visual interpretation in 46 randomly selected windows of 5 km × 5 km (166 × 166 Landsat pixels) covering the nine major classes (figure 3). The Landsat estimates were for total irrigated area only, and did not separate surface- and groundwater-irrigated areas. A total of 16 Landsat scenes cover the Krishna Basin. GeoCover 2000 acquisition dates differed for each scene, but were mostly in late October to early December in the mid-late monsoon (Kharif) cropping season. Two GeoCover

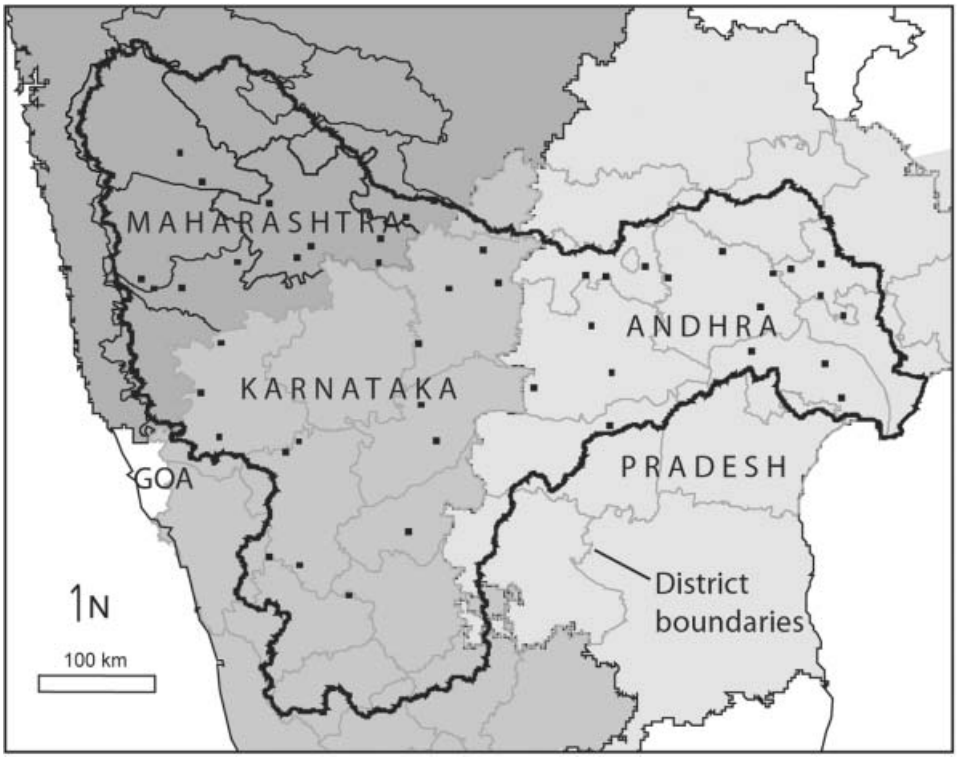

Figure 3. State and district boundaries in the Krishna Basin. The small black squares are the 5 km × 5 km sample areas used for irrigated fraction estimates from Landsat TM imagery.

2000 images acquired in February 2001 were excluded from the irrigated area estimation.

3.3 *Accuracy assessment: fuzzy and irrigation fraction approaches*

Traditional accuracy assessment determines the probability that the class assigned to a pixel matches ground truth data at the same location. For imagery with significant sub-pixel heterogeneity in land cover and for mapping large areas, this kind of accuracy assessment is difficult and potentially misleading (Friedl *et al.* 2000, Latifovic and Olthof 2004). Point sampling is usually feasible for only a small fraction of the basin area, even with intensive fieldwork. In the Krishna Basin ground truth campaign, a total of 140 points of 0.25 km^2 each were sampled, covering 0.0001% of the basin area. Realistically, this is often best done in remote sensing field work at regional scales; sampling 140 points took 22 days travelling nearly 6500 km. Here, we implemented two alternative approaches to accuracy assessment for a large area with sub-pixel heterogeneity: a fuzzy estimate that measured different degrees of correctness over a pixel window, and a comparison of irrigated fractions using the three methods described in section 3.2 (GT, ML, and TM).

Fuzzy accuracy assessment is appropriate where land cover is heterogeneous (Gopal and Woodcock 1994, Thenkabail *et al.* 2005). Here we used a 3 × 3 MODIS pixel window around each ground truth point and determined the average correctness in each window. Each cell in the 3 × 3 window received a score of

Table 2. Scores applied in the fuzzy accuracy assessment. Percent correct for each 3×3 pixel window is the average score of the nine pixels.

		MODIS class								
		WAT	RL	RFA	RFG	IMIN	IL	IDBL	ICONT	FOR
Ground-truth class	WAT	100	0	0	0	0	0	0	0	0
	RL	0	100	50	0	0	0	0	0	0
	RFA	0	50	100	50	50	0	0	0	0
	RFG	0	0	50	100	50	50	50	50	0
	IMIN	0	0	50	50	100	50	50	50	0
	IL	0	0	0	50	50	100	50	50	0
	IDBL	0	0	0	50	50	50	100	50	0
	ICONT	0	0	0	50	50	50	50	100	0
	FOR	0	0	0	0	0	0	0	0	100

100% correct if the MODIS class matched the ground truth class (table 2). The cell received a score of 50% correct if the MODIS class differed from the ground truth category, but still had some degree of accuracy, such as when a minor irrigated MODIS class pixel had a ground truth label of rainfed-groundwater irrigated. The percent correct for a window around a given ground truth point was the average of the scores of the nine cells. Windows with a score of 100% correct received a label 'Absolutely correct,' those with a score of 75–99% had a label of 'Mostly correct' and so on (table 3).

The fuzzy method sometimes labeled correctly classified pixels as incorrect, because heterogeneity in land cover occurred over the $1500\,\text{m} \times 1500\,\text{m}$ area surrounding each ground truth point. This was offset by giving a 50% correct score to similar classes. Most classes had mixed land cover, so in numerous cases a 50% correct score was applied, which likely overestimated accuracy in some cases. The fuzzy method did not test the accuracy of sub-pixel irrigated fractions or total irrigated area of each class, but rather gave a first indication of the match between the ground truth data and the MODIS classification.

Aggregate accuracy was also assessed by comparing the irrigated fractions determined from the ground truth data (GT method), district agricultural census data (ML method) and Landsat TM imagery (TM) as described in section 3.2. Comparison of the three methods for obtaining irrigated fractions (GT, ML, and TM) either increased confidence in the irrigated fraction of a class, or identified particularly challenging classes that require further fieldwork for determination of the irrigated fraction.

3.4 *Vegetation phenology from NDVI time series*

The dates of vegetation transitions were determined using the NDVI time series and a double-logistic model of vegetation phenology (Fischer 1994):

$$NDVI(t) = v_b + \frac{k}{1+\exp(-c(t-p))} - \frac{k+v_b-v_e}{1+\exp(-d(t-q))} \quad (2)$$

where v_b and v_e are the NDVI at the beginning and end of the growing season, k is an asymptotic maximum value of NDVI, c and d are the slopes of the NDVI time series at the inflection points, and p and q are the dates of the inflection points (figure 4). The beginning of the time series was defined as the date of minimum

Table 3. Fuzzy accuracy assessment using ground truth data. Numbers in parentheses indicate the fuzzy correctness percentage. Values in the table are the percentages of ground truth windows in given class having a given correctness.

Map code	Class name	TOTAL correct (51–100%)	TOTAL incorrect (0–50%)	Absolutely correct (100%)	Mostly correct (76–99%)	Partly correct (51–75%)	Partly incorrect (26–50%)	Mostly incorrect (1–25%)	Absolutely incorrect (0%)
WAT	Water	100	0	100	0	0	0	0	0
RL	Rangeland	72	28	31	14	27	25	3	0
RFA	Rainfed agriculture	85	15	30	35	20	15	0	0
RFG	Rainfed + gw irrigation	61	39	33	6	22	21	2	16
IMIN	Minor irrigation	80	20	0	62	18	17	0	3
IL	Irrigated, low NDVI	81	19	56	9	17	17	1	0
ICONT	Continuous irrigation	68	32	46	8	14	14	0	18
IDBL	Irrigated double crop	80	20	79	0	1	20	0	0
FOR	Forest	66	34	63	3	0	27	0	7
Total	All classes	77	23	49	15	13	17	1	5

NDVI within a 3-month window prior to the monsoon (April–June). The onset and termination of the growing season may be defined in a number of different ways (Kang *et al*. 2003). We used the definition of Zhang *et al*. (2003), where the maximum changes in curvature of the NDVI time series function define transition dates, i.e. the maxima and minima of the third derivative of equation (2) (figure 4).

In order to determine the parameter values of equation (2), the 8-day composite NDVI time series was masked for clouds using a simple threshold procedure (Thenkabail *et al*. 2005), and the NDVI time series determined for each of the 37 classes. The NDVI curves for each class were further cleaned for residual cloud and haze effects by removing dates with a large, single-date drop in NDVI. Equation (2) was fitted to the observed NDVI time series using a multidimensional, unconstrained nonlinear error minimization algorithm (Nelder–Mead Simplex method, Matlab v5.3). Note that the vegetation transition dates were not used for the classification, but rather quantified vegetation phenology and cropping calendars of each class.

4. Results and discussion

4.1 *Land cover classification and irrigated fractions*

The unsupervised classification based on the MODIS NDVI time series had nine generalized classes (figure 5, table 1). Rangelands (RL, 24% of total basin area), mixed rainfed-groundwater irrigation (RFG, 24%), and rainfed agriculture (RFA, 20%) dominated the basin area, followed by minor irrigation, which included a mixture of rainfed ecosystems, small reservoirs, riparian lift irrigation, and groundwater irrigation (IMIN, 14%). Forest (FOR) covered 5.9% of the basin area.

Classes irrigated by surface water (11% of total basin area), included continuous irrigation (ICONT, 3.3%), double crop irrigated (IDBL, 4.5%), and light irrigation

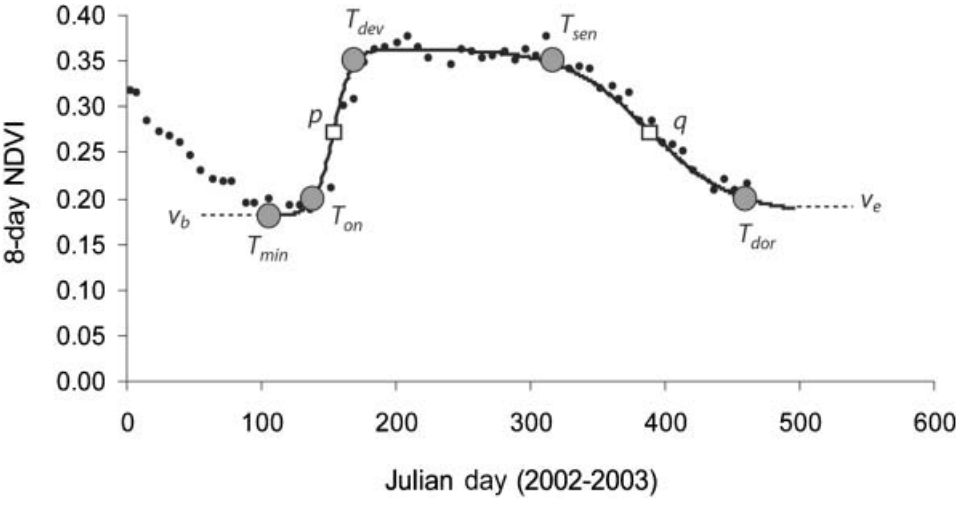

Figure 4. Logistic model of vegetation phenology and transition dates, as in equation (2). T_{min} defines the beginning of the time series, T_{on} is onset of greenness, T_{dev} beginning of development stage, T_{sen} onset of senescence, and T_{dor} is termination of senescence. p and q are the inflection points. The black dots indicate the observed 8-day NDVI time series for one of the 37 sub-classes (Rangeland). v_b and v_e are the NDVI at the beginning and end of the growing season, respectively.

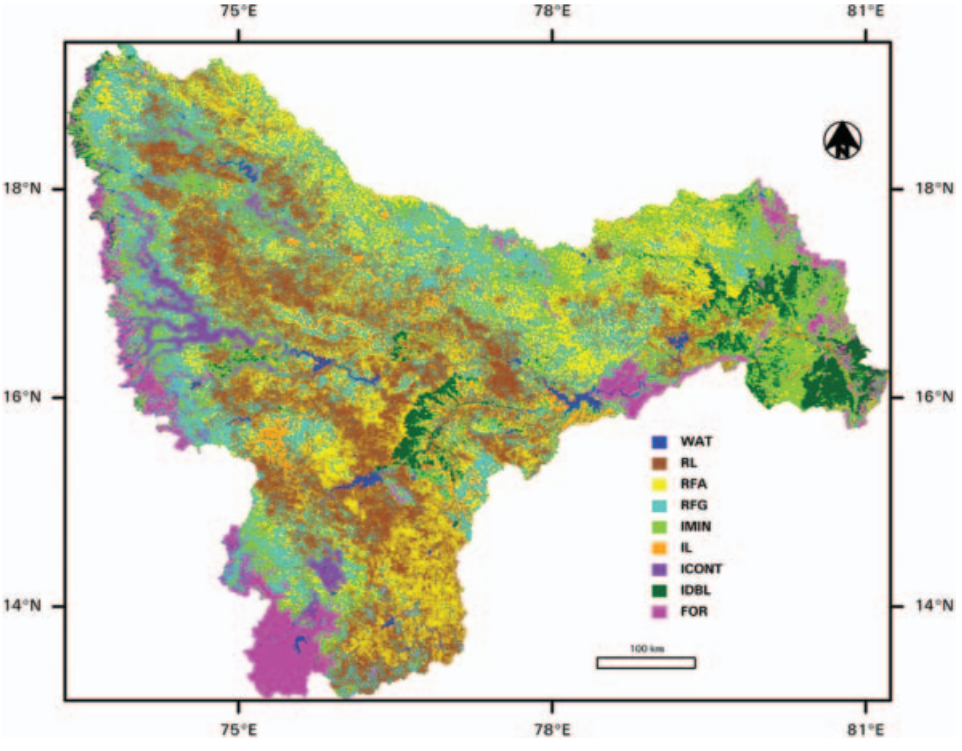

Figure 5. Land cover map of the Krishna Basin from the MODIS NDVI classification. WAT=water bodies; RL=rangeland/rainfed crops; RFA=rainfed agriculture; RFG=mixed rainfed crops and groundwater irrigation; IMIN=minor irrigation from lift, tanks, and groundwater; IL=canal irrigated, low NDVI; ICONT=irrigated continuous; IDBL=irrigated double crop; FOR=forests (evergreen, deciduous, agroforest, and mixed shrubs). See table 1 for vegetation cover statistics, and table 4 for the irrigated fraction of each class.

with low NDVI and late onset of greening (IL, 3.0%). These three classes mapped large, contiguous irrigated areas served by major reservoirs and canals, medium irrigation projects and other pixels dominated by continuous or double-cropping. ICONT had continuous or near-continuous irrigation and included sugarcane cultivation in the north-west and central-west parts of the basin (figure 5), and a mixture of rice and plantations in the Tunga command area in the south (TN in figure 1). IDBL included rice–rice and rice–grains in major irrigated systems on the Tungabhadra (TB in figure 1), Nagarjuna Sagar (NJS) and the delta (KD). The lower NDVI in April–May in IDBL resulted from fallows prior to the monsoon. The IL class occurred in a large contiguous area in the western part of the basin (MP in figure 1), along the fringes of major irrigated command areas, and in several small patches along river corridors (figure 5). IL had relatively low NDVI compared with ICONT and IDBL, likely due to more fragmented plots, lower irrigation intensity, and a crop mix that included cotton and oilseeds. Forest classes (FOR) had the highest annual-average NDVI, followed by continuous irrigation (ICONT), double-cropped irrigated (IDBL), minor irrigation (IMIN), rainfed and groundwater (RFG), and rainfed agriculture (RFA) and rangelands (RL) (figures 6 and 7). The surface water-irrigated classes had larger and more spatially uniform irrigated areas

than the IMIN and RFG classes, which had intermixed and patchy irrigated and rainfed systems (figure 5).

All classes represent a mix of different cover types, so the class names indicate dominance of a particular cover and not a pure class. The RL and RFA classes included both rangeland and rainfed cropping, which were difficult to separate given their similar vegetation phenology. Irrigated classes, especially RFG and IMIN, included heterogeneous mosaics of irrigation from different sources (surface and groundwater), rainfed crops, and rangelands.

Tree cover was low for the basin as a whole (~5%, table 1), and crops dominated most class areas. The forest class (FOR) had a low percentage of trees and shrubs (39%), with nearly 60% grass, weeds, and open/bare. Despite low tree and shrub cover, the class was labeled following the FAO/UNEP definition of forest, which includes temporary clearings that are expected to regenerate to forest cover (FAO/UNEP 1999). The vegetation cover percentages based on the GT data all had high standard deviations, so uncertainty remains high around some of the basin-scale cover estimates.

Seventy-seven percent of the 3×3 windows around the ground truth points classified as ''Correct'' or better in the fuzzy accuracy assessment (table 3). The

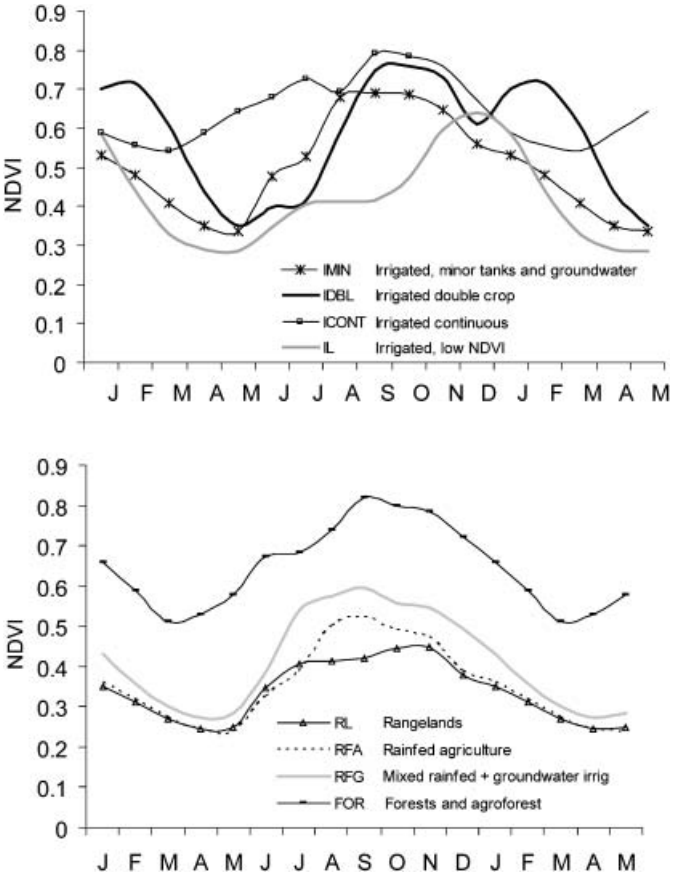

Figure 6. NDVI time series for the generalized classes in figure 5, excluding the water bodies class corresponding to the classified image in figure 5. Maximum-value composite images were available only for 2002, so January to May are represented twice in the figure.

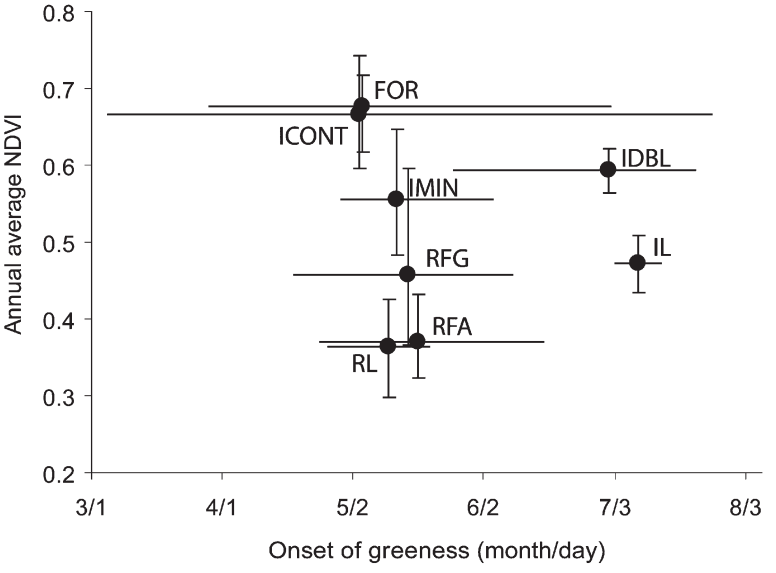

Figure 7. Onset of greenness versus annual mean NDVI for the MODIS classes. The bars represent the minimum and maximum for each of the 37 sub-classes within each of the 9 generalized classes.

surface irrigated classes (IDBL, ICONT, IL) had relatively high correctness (68–81%). Combining the three surface irrigated classes into a single class increased the accuracy to 90%. The RFG class had the lowest accuracy (61% correct or better), and the RL and RFA classes had the highest accuracy (85% correct or better).

4.2 *Irrigated fractions*

The three major irrigated classes (IDBL, ICONT, IL) had statistically significant irrigated fractions when regressed against surface water irrigated area from the census in the ML method (table 4). The double cropped irrigated class (IDBL) had a higher irrigated fraction ($\alpha_{i,k}=0.79$) than the continuous irrigated (ICONT) and irrigated with low NDVI classes (IL) ($\alpha_{i,k}=0.51$ and 0.49, respectively). A single class, RFG, accounted for most of the variance in groundwater irrigated area from the agricultural census ($R^2=0.69$, $p<0.0001$). The irrigated fraction for the IMIN class was weakly significant ($p<0.056$). The $\alpha_{i,k}$ for all other classes were not statistically different from zero ($p>0.1$). Two outlier districts (figure 8) were excluded from the ML regression for the groundwater-irrigated fraction in order to make the regression representative for the majority of the basin area.

All three methods (GT, ML, TM) gave similar estimates of the irrigated fractions for surface irrigated area and total irrigated area (table 4). For the surface-irrigated classes (IDBL, ICONT, IL), the area fraction irrigated by surface water was nearly the same for the GT ($\alpha=0.65$) and ML methods ($\alpha=0.59$). Total irrigated fractions ranged from 0.25 to 0.26 for the RFG class, and between 0.51–0.68 and 0.61–0.79 for the ICONT and IDBL classes, respectively. The IMIN class showed the widest discrepancy among the three methods (α range 0.09–0.43). Groundwater-irrigated fractions differed more widely by method than surface or total irrigated fractions. The groundwater-irrigated fraction for RFG determined using ML (0.25) exceeded the GT estimate by more than three times (0.07).

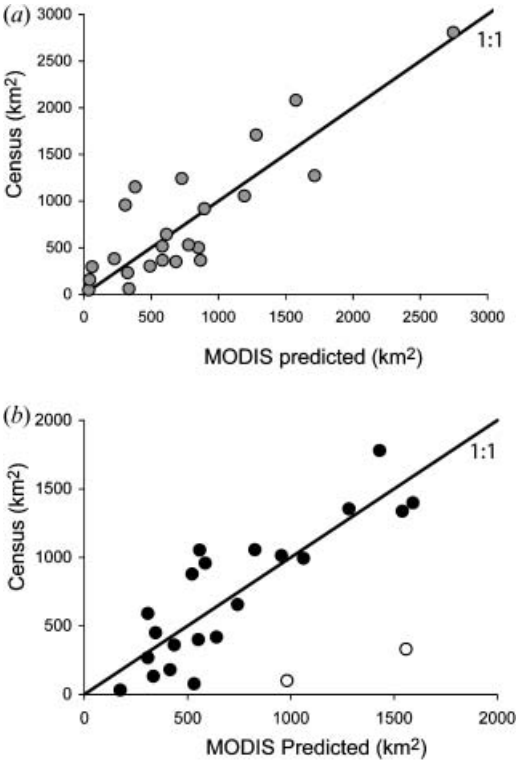

Figure 8. District-wise irrigated area from the MODIS classification compared with the agricultural census, for areas irrigated by (*a*) surface water and (*b*) groundwater. The multiple regression (ML) method was used for calculating irrigated fractions and irrigated areas. White circles in the groundwater irrigated area chart indicate two outlier districts excluded from the multiple regression.

The GT method gave the highest estimate of basin-total irrigated area due to the high irrigated fraction estimate in the IMIN class (table 4). The basin-total irrigated area for all irrigated classes excluding IMIN differed by less than 15% (GT = 37 747 km^2, ML = 33 200 km^2, and TM = 36 344 km^2). This highlighted the uncertainty around the irrigated fraction of the IMIN class, and the agreement among the three methods for all other classes. The large differences in the irrigated fraction of the IMIN class as estimated by the GT, ML, and TM methods could be due to several reasons, including: (1) the small plot sizes of irrigated areas common in the IMIN class. More than 60% of the area irrigated with shallow tube wells in Andhra Pradesh occurred on plots smaller than 2 ha, or 141m on a side (Government of India 2001). A 500 m × 500 m pixel covered 25 ha and so may have contained several groundwater irrigated pixels (figure 2). However, the relatively good correlation between groundwater irrigated area estimated by MODIS and the agricultural census (figure 8) suggests that broad groundwater classes and their areas were mapped correctly. (2) The definition of groundwater and surface water irrigation in the GT data likely accounted for some differences between the GT and ML estimates of the irrigated fractions. Tank-irrigated systems included areas irrigated by dug wells or tube wells, and many tank systems were used primarily to recharge aquifers for groundwater irrigation. These systems were counted as surface-irrigated in the ground truth statistics, which caused underestimation of the

Table 4. Net irrigated fractions ($\alpha_{i,k}$) and net irrigated areas ($I_{i,k}$) by class, determined by ground truth data (GT), multiple-regression on agricultural census data (ML), and Landsat TM imagery (TM). All reported values of α for the ML method were statistically different from zero at $p<0.1$. n.s. indicates $p>0.1$.

Class name	Rangeland	Rainfed agriculture	Rainfed + Groundwater irrigation	Minor irrigation	Irrigation, low NDVI	Continuous irrigation	Irrigated double crop	
Map code	RL	RFA	RFG	IMIN	IL	ICONT	IDBL	Basin total
			Irrigated fraction $\alpha_{i,.}$					
Ground water $\alpha_{i,g}$								
GT	0.02	0.03	0.07	0	0.05	0.04	0.07	0.03
ML	n.s.	n.s.	0.25	0.09	n.s.	n.s.	n.s.	0.07
Surface water $\alpha_{i,s}$								
GT	0	0	0.18	0.43	0.69	0.64	0.62	0.18
ML	n.s.	n.s.	n.s.	n.s.	0.49	0.51	0.79	0.07
Total irrigated fraction $\alpha_{i,g}+\alpha_{i,s}$								
GT	0.02	0.03	0.25	0.43	0.74	0.68	0.69	0.21
ML	n.s.	n.s.	0.25	0.09	0.49	0.51	0.79	0.14
TM	0.02	0.09	0.26	0.20	0.33	0.51	0.61	0.17
			Total class area and irrigated area ($I_{i,k}$), in km^2					
Total class area (km)^2	63 143	51 162	62 944	35 788	7702	8600	11 775	258 912
Ground water $I_{i,g}$								
GT	1004	1660	4080	0	511	413	419	8080
ML	0	0	15 740	3220	0	0	0	18 960
Surface water $I_{i,s}$								
GT	0	0	11 300	11 500	4790	5500	8070	45 500
ML	0	0	0	0	3770	4390	9300	17 460
Total irrigated $I_{i,g}+I_{i,s}$								
GT	1004	1660	15 380	11 500	5301	5913	8489	53 580
ML	0	0	15 740	3220	3770	4390	9300	36 520
TM	1263	4605	16 365	7158	2542	4386	7183	43 501

groundwater-irrigated fraction. (3) Under-sampling of groundwater irrigation and over-sampling of surface irrigated systems may have occurred during collection of ground truth data. Homogeneous areas of at least 500 m × 500 m were chosen for ground truth points. This may have caused over-sampling of large, homogenous surface water-irrigated systems and under-sampling of small and spatially discontinuous groundwater-irrigated plots.

The results from all three methods for determining the irrigated fractions (GT, ML, TM) highlighted the importance of groundwater and minor irrigation, which has also been noted for irrigation in India as a whole (Shah *et al*. 2000). The total irrigated area in the rainfed and minor irrigated classes (RL, RFA, RFG, IMIN) exceeded the irrigated area in major irrigated classes (IL, ICONT, IDBL) for all three methods (figure 9). These heterogeneous classes dominated by smallholder agriculture represent a continuing challenge for irrigated area mapping with coarse resolution imagery. The combination of ground truth, census data, and high-resolution imagery used here helped constrain the uncertainty in irrigated area and irrigated fractions.

4.3 *Vegetation phenology of groundwater and surface water irrigation*

Groundwater and surface water irrigation showed good separation in the classification, and district-wise irrigated area from the classification compared well with district-level census data (figure 8). Two properties of the NDVI time series allowed separation of areas irrigated by groundwater and surface water: annual average NDVI, which was a function of the irrigated fraction, and timing of the onset of greenness, which was a function of the timing of water delivery. Annual NDVI in both continuous and double irrigated systems exceeded annual NDVI in groundwater systems, reflecting the higher irrigated fraction in areas irrigated with surface water. Double cropped (IDBL) and irrigated with low NDVI (IL) classes had relatively late onset of greenness, because they were irrigated by canal water from reservoirs that drain large catchments and take weeks or months to fill. Minor irrigation and groundwater-irrigated areas had early onset of greenness because aquifers provide water prior to and shortly following the onset of rains, and small reservoirs drain smaller watersheds and fill more quickly (figure 7).

Groundwater and surface water-irrigated areas also tended to be spatially segregated, which enhanced their separability. Groundwater irrigation occurred along valley bottoms of second and third order streams or below small reservoirs, while surface irrigation occurred below major reservoirs draining large areas. Conjunctive use of surface and groundwater may occur in some areas, such as in minor schemes near small reservoirs, in sugarcane irrigated areas during the dry season, or at the tail end of canals in surface water commands areas. However, clear and quantitative separation of the two sources in major canal command areas was difficult, even in the field. In the MODIS classification, areas of conjunctive irrigation were put in surface water-irrigated classes.

4.4 *Comparison of present method with other mixed-pixel analyses*

The use of unsupervised classification and aggregate irrigated fractions differs from other mixed-pixel methods such as linear-mixture modeling, which assign different fractional cover to each pixel in an image based on proximity to pre-defined endmembers in spectral space (Shiambukuro and Smith 1991, Quarmby *et al*. 1992,

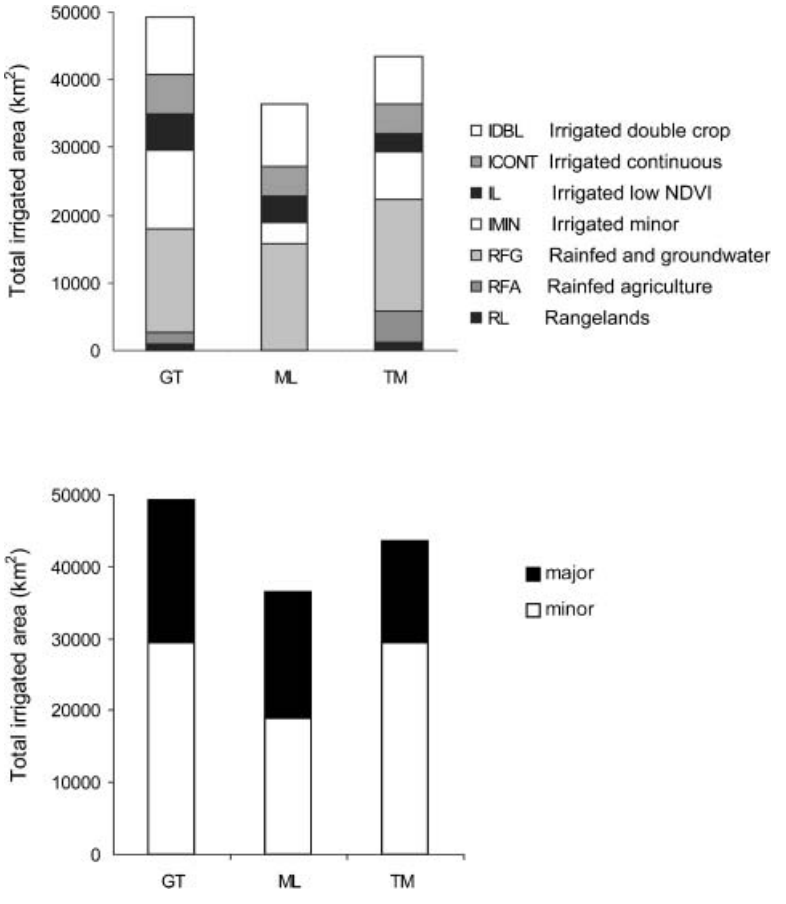

Figure 9. Basin irrigated area compared for the three different methods for determining the irrigated fractions. GT indicates ground truth method, ML is multiple regression on census data, and TM is Landsat TM imagery. Minor irrigation is the sum of irrigated area in the rangeland (RL), rainfed agriculture (RFA), rainfed plus groundwater irrigation (RFG), and minor irrigation (IMIN) classes. Major irrigation is the sum of irrigated area in irrigated low NDVI (IL), continuous irrigation (ICONT), and irrigated double crop (IDBL) classes.

Holben and Shimabukuro 1993, DeFries *et al.* 2000, Roberts *et al.* 2002). The multiple regression component of our approach resembles other studies that disaggregate agricultural census data using satellite imagery over large areas (Ramankutty and Foley 1998, Frolking *et al.* 2002). We used a combination of unsupervised classification and aggregate irrigated fractions instead of supervised classification or pixel-wise endmember mixing models for four main reasons. First, the selection of endmembers or supervised training sites that applied over the whole image was difficult over the large basin given its diverse climate, vegetation, and cropping patterns. The small size of many irrigated plots and the diversity of irrigation practices, including variations in cropping calendars within a class, complicated selection of meaningful endmembers on coarse resolution imagery. Second, limited ground truth data (144 samples over a large basin) precluded identification of all important irrigation classes. The IL class, for example, had a distinct NDVI signature and cropping pattern, but was visited at only four locations in the field campaign. The unsupervised classification allowed for identification and

mapping of the full range of vegetation and irrigation types, including those not visited during the rapid field campaign. Third, irrigated classes with low irrigated fractions (e.g. RFG, IMIN) had NDVI time series similar to rainfed classes. An endmember approach that scaled irrigated area to NDVI overestimated the irrigated area in rainfed areas with vigorous vegetation, and underestimated the irrigated area in sparsely irrigated classes in arid areas. For these reasons, unsupervised classification and an aggregate irrigated fraction were used instead of supervised classification or endmember mixing models.

The main disadvantage of the method was dependence of the class merging procedure on user experience. The class merging procedure required qualitative comparison of NDVI time series, Landsat TM imagery, and ground truth data by a user experienced with land cover and irrigation systems in the region. Subtle differences among classes that differed only slightly in irrigated fraction or vegetation vigor resulted in several different merging outcomes, depending on user judgment. Automated merging of classes using the NDVI time series and some distance metric (e.g. Cihlar *et al*. 1998) was not possible, since some distinct classes differed only slightly in their NDVI time series. The method was therefore only partially automated, and different user interpretations of class merging could result in different irrigated area maps. Nevertheless, the overall correlation between the MODIS irrigated area and the census data demonstrated the benefit of comparing multiple data sources for irrigated area mapping in a complex landscape.

4.5 *Application of the method in other regions and time periods*

The MODIS classification covered a large basin with a range of climates, from semi-arid in the central basin to humid in the Western Ghats. The technique had most success in semi-arid to arid environments where irrigation had a strong impact on vegetation phenology. Areas with high rainfall ($>$1000 mm) and vigorous natural vegetation were easily confused with irrigated areas, particularly if irrigation was for a single crop as in groundwater irrigated areas. The largest classification errors occurred in the high rainfall areas in the Western Ghats, where forests, irrigated sugarcane, and rice mixed spatially and had similar NDVI signatures. Errors were also high in minor irrigated areas of the eastern part of the basin, where irrigated patches were small and vegetation phenology of irrigated systems was similar to rainfed systems. Where irrigated patches cover a small fraction of a pixel, robust estimation of the irrigated fraction remains challenging. Humid areas had the additional challenge of cloud cover, which obscured mapping during some of the most important periods of vegetation and crop development.

The separation of groundwater and surface water irrigation depended on the delay in surface water supply for irrigation. This delay is expected to be largest where surface irrigated schemes receive water from large catchment areas that have long delays between the onset of rainfall, reservoir filling, and canal releases. Seperation of groundwater and surface water irrigated areas would be difficult with the present method in areas having conjunctive use, unless the timing of planting differed between the two types of irrigation.

5. Conclusions

A MODIS NDVI time series was combined with ground truth data, agricultural census data, and Landsat TM to map surface water irrigation, groundwater

irrigation, and rainfed ecosystems in a region of India dominated by smallholder agriculture. The irrigated fraction approach was used to map heterogeneous and patchy irrigated areas, including the groundwater and minor irrigated areas that dominated basin irrigated area. The combination and comparison of multiple data sources yielded robust estimates of irrigated fractions and identified classes with high uncertainty, in particular minor irrigated areas in areas of high rainfall. The unsupervised classification of the NDVI time series identified and separated different types of irrigation including double cropped grains, continuous irrigation, irrigated areas with low vegetation vigor, and minor and groundwater irrigation. Differences in timing of greening allowed separation of groundwater and surface water irrigation where the two were spatially segregated. A distinct advantage of the NDVI time series method was its simplicity and ease of application for other areas, though significant user interaction and field experience was required for an accurate map. Given the importance of small irrigated patches for total basin irrigated area, especially in developing countries such as India, use of an irrigated fraction approach is recommended for future regional mapping efforts.

Acknowledgments

Thanks to Dr. David Molden and Professor Frank Rijsberman of the International Water Management Institute (IWMI) who facilitated financial support from the Government of the Netherlands through the IWMI-led Comprehensive Assessment of Water Management in Agriculture, the Government of Japan, and the Australian Centre for International Agricultural Research. Two anonymous reviewers provided thorough comments and helpful suggestions.

References

ACHARD, F. and ESTREGUIL, C., 1995, Forest classification of Southeast Asia using NOAA AVHRR data. *Remote Sensing of Environment*, **54**, pp. 198–208.

CARDILLE, J.A. and FOLEY, J.A., 2003, Agricultural land-use change in Brazilian Amazonia between 1980 and 1995: evidence from integrated satellite and census data. *Remote Sensing of Environment*, **87**, pp. 551–562.

CIHLAR, J., XIAO, Q., BEAUBIEN, J., FUNG, K. and LATIFOVIC, R., 1998, Classification by progressive generalization: a new automated methodology for remote sensing multichannel data. *International Journal of Remote Sensing*, **19**, pp. 2685–2704.

CIHLAR, J., 2000, Land cover mapping of large areas from satellites: status and research priorities. *International Journal of Remote Sensing*, **21**, pp. 1093–1114.

DEFRIES, R.S., HANSEN, M., TOWNSHEND, J.R.G. and SOHLBERG, R., 1998, Global land cover classifications at 8 km spatial resolution: the use of training data derived from Landsat imagery in decision tree classifiers. *International Journal of Remote Sensing*, **19**, pp. 3141–3168.

DEFRIES, R.S., HANSEN, M. and TOWNSHEND, J., 2000, Global continuous fields of vegetation characteristics: a linear mixture model applied to multiyear 8 km AVHRR data. *International Journal of Remote Sensing*, **21**, pp. 1389–1414.

DEFRIES, R.S. and TOWNSHEND, J.R.G., 1994, NDVI-derived land cover classifications at a global scale. *International Journal of Remote Sensing*, **15**, pp. 3567–3586.

DROOGERS, P., 2002, *Global Irrigated Area Mapping: Overview and Recommendations. Working Paper 36* (Colombo, Sri Lanka: International Water Management Institute).

FAO/UNEP, 1999, *Terminology for Integrated Resources Planning and Management* (Rome, Italy and Nairobi, Kenya: Food and Agriculture Organization/United Nations Environmental Programme).

FISCHER, A., 1994, A model for the seasonal variations of vegetation indices in coarse resolution data and its inversion to extract crop parameters. *Remote Sensing of Environment*, **48**, pp. 220–230.

FRIEDL, M.A., WOODCOCK, C., GOPAL, S., MUCHONEY, D., STRAHLER, A.H. and BARKER-SCHAAF, C., 2000, A note on procedures used for accuracy assessment in land cover maps derived from AVHRR data. *International Journal of Remote Sensing*, **21**, doi 10.1080/014311600210434.

FROLKING, S., QIU, J.B.S., XIAO, X., LIU, J., ZHUANG, Y., LI, C. and QIN, X., 2002, Combining remote sensing and ground census data to develop new maps of the distribution of rice agriculture in China. *Global Biogeochemical Cycles*, **16**, doi 10.1029/2001GB001425.

GOPAL, S. and WOODCOCK, C., 1994, Theory and methods for accuracy assessment of thematic maps using fuzzy sets. *Photogrammetric Engineering and Remote Sensing*, **60**, pp. 181–188.

GOVERNMENT OF INDIA, 2001, *Report on Census of Minor Irrigation Schemes—1993–94* (Delhi: Ministry of Water Resources, Minor Irrigation Division).

GUILMOTO, C.Z., 2002, Irrigation and the great Indian rural database: vignettes from South India. *Economic and Political Weekly*, **37**, pp. 1223–1228.

HILL, M.J. and DONALD, G.E., 2003, Estimating spatio-temporal patterns of agricultural productivity in fragmented landscapes using AVHRR NDVI time series. *Remote Sensing of Environment*, **84**, pp. 367–384.

HOLBEN, B.N., 1986, Characteristics of maximum-value composite images from temporal AVHRR data. *International Journal of Remote Sensing*, **7**, pp. 1417–1434.

HOLBEN, B.N. and SHIMABUKURO, Y.E., 1993, Linear mixing model applied to coarse spatial resolution data from multispectral satellite sensors. *International Journal of Remote Sensing*, **14**, pp. 2231–2240.

HUETE, A., DIDAN, K., MIURA, T. and RODRIGUEZ, E., 2002, Overview of the radiometric and biophysical performance of the MODIS vegetation indices. *Remote Sensing of Environment*, **83**, pp. 195–213.

KANG, S., RUNNING, S.W., LIM, J.H., ZHAO, M., PARK, C.R. and LOEHMAN, R., 2003, A regional phenology model for detecting onset of greenness in temperate mixed forests, Korea: an application of MODIS leaf area index. *Remote Sensing of Environment*, **86**, pp. 232–242.

KING, M.D., CLOSS, J., SPANGLER, S. and GREENSTONE, R. (Eds) 2003, *EOS Data Products Handbook Version 1* (Greenbelt, MD: NASA Goddard Space Flight Center).

LATIFOVIC, R. and OLTHOF, I., 2004, Accuracy assessment using sub-pixel fractional error matrices of global land cover products derived from satellite data. *Remote Sensing of Environment*, **90**, pp. 153–165, doi:110.1016/j.rse.2003.1011.1016.

LLOYD, D., 1990, A phenological classification of vegetation cover using shortwave vegetation index imagery. *International Journal of Remote Sensing*, **11**, pp. 2269–2279.

MOODY, A. and JOHNSON, D.M., 2001, Land-surface phenologies from AVHRR using the discrete Fourier transform. *Remote Sensing of Environment*, **75**, pp. 305–323.

QUARMBY, N.A., TOWNSHEND, J.R.G., SETTLE, J.J., WHITE, K.H., MILNES, M., HINDLE, T.L. and SILLEOS, N., 1992, Linear mixture modeling applied to AVHRR data for crop area estimation. *International Journal of Remote Sensing*, **13**, pp. 415–425.

RAMANKUTTY, N. and FOLEY, J.A., 1998, Characterizing patterns of global land use: an analysis of global croplands data. *Global Biogeochemical Cycles*, **12**, pp. 667–685.

REED, B.C., BROWN, J.F., VANDERZEE, D., LOVELAND, T.R., MERCHANT, J.W. and OHLEN, D.O., 1994, Measuring phenological variability from satellite imagery. *Journal of Vegetation Science*, **5**, pp. 703–714.

ROBERTS, D.A., NUMATA, I., HOLMES, K., BATISTA, G., KRUG, T., MONTEIRO, A., POWELL, B. and CHADWICK, O.A., 2002, Large area mapping of land-cover change in Rondônia using multitemporal spectral mixture analysis and decision tree classifiers. *Journal of Geophysical Research*, **107**, pp. 8073, JD000374.

ROSENBERG, D.M., 2000, Global-scale environmental effects of hydrological alterations. *BioScience*, **50**, pp. 746–751.

SELLERS, P.J. and SCHIMEL, D., 1993, Remote sensing of the land biosphere and biogeochemistry in the EOS era: science priorities, methods and implementation. *Global and Planetary Change*, **7**, pp. 279–297.

SHAH, T., MOLDEN, D., SAKTHIVADIVEL, R. and SECKLER, D., 2000, *The Global Groundwater Situation: Overview of Opportunities and Challenges* (Colombo, Sri Lanka: International Water Management Institute).

SHIKLOMANOV, I.A., 2000, Appraisal and assessment of world water resources. *Water International*, **25**, pp. 11–32.

SHIMABUKURO, Y.E. and SMITH, J.A., 1991, The least-squares mixing models to generate fraction images derived from remote sensing multispectral data. *IEEE Transactions on Geoscience and Remote Sensing*, **29**, pp. 16–20.

THENKABAIL, P., SCHULL, M. and TURRAL, H., 2005, Ganges and Indus river basin land use/land cover (LULC) and irrigated area mapping using continuous streams of MODIS data. *Remote Sensing of Environment*, **95**, pp. 317–341.

TUCKER, C.J., GRANT, D.M. and DYKSTRA, J.D., 2004, NASA's global orthorectified Landsat data set. *Photogrametric Engineering and Remote Sensing*, **70**, pp. 313–322.

WALKER, P.A. and MALLAWAARACHICHI, T., 1998, Disaggregating agricultural statistics using NOAA-AVHRR NDVI. *Remote Sensing of Environment*, **63**, pp. 112–125.

WARDLOW, B.D. and EGBERT, S.L., 2002, Discriminating cropping patterns for the U.S. central Great Plains region using time-series MODIS 250m NDVI data—preliminary results. In *Integrated Remote Sensing at the Global, Regional and Local Scale*, 10–15 November 2002, Denver, CO.

ZHANG, X., FRIEDL, M.A., SCHAAF, C.B., STRAHLER, A.H., HODGES, J.C.F., GAO, F., REED, B.C. and HUETE, A., 2003, Monitoring vegetation phenology using MODIS. *Remote Sensing of Environment*, **84**, pp. 471–475.